

# Tunable multiple layered Dirac cones in optical lattices

Z. Lan,<sup>1</sup> A. Celi,<sup>2</sup> W. Lu,<sup>1</sup> P. Öhberg,<sup>1</sup> and M. Lewenstein<sup>2,3</sup>

<sup>1</sup>*SUPA, Department of Physics, Heriot-Watt University, EH14 4AS, Edinburgh, United Kingdom*

<sup>2</sup>*ICFO The Institute of Photonic Sciences Av. Carl Friedrich Gauss, num. 3, E-08860 Castelldefels (Barcelona), Spain*

<sup>3</sup>*ICREA-Institució Catalana de Recerca i Estudis Avançats, 08010 Barcelona, Spain*

We show that multiple layered Dirac cones can emerge in the band structure of properly addressed multi-component cold fermionic gases in optical lattices. The layered Dirac cones contain multiple copies of the massless spin-1/2 Dirac fermions at the *same* location in momentum space, whose different Fermi velocity can be tuned at will. On-site microwave Raman transitions can further lead to the mixing of the different Dirac species, resulting in a splitting of the multiple layered cones into several single layered cones. The tunability of the multiple layered Dirac cones allows to simulate a number of fundamental phenomena in modern physics, such as neutrino oscillations and exotic particle dispersions with  $E \sim p^n$  for arbitrary integer  $n$ .

PACS numbers: 37.10.Jk, 71.10.Fd, 71.15.Rf, 14.60.Pq

**Introduction.** The concept of a quantum emulator was first introduced by Feynman as a way to avoid the difficulty of simulating quantum phenomena with classical computers [1]. The idea was to use one controllable system to simulate another, possibly computationally intractable system. Nowadays Feynman's intuition is being implemented in various setups and among them, cold gases of neutral atoms play a central role [2, 3]. Systems of trapped ultracold atoms in optical lattices have proven to be a remarkable tool for simulating a vast range of condensed matter, and lately also high energy physics phenomena. Graphene and topological insulators have recently attracted a significant attention due to their massless low-energy excitations, termed Dirac fermions, which govern the electron transport properties [4, 5]. They are examples of quasi-relativistic dynamics in a non-relativistic environment. In an effort to extend such behavior to quasi-particles with arbitrary spin, a quantum simulator of the so called Dirac-Weyl fermions with arbitrary large spin [6] has been proposed. This can be implemented by using multicomponent cold fermionic atoms trapped in an optical lattice, and by tuning the hopping matrices between these internal states according to  $\mathfrak{su}(2)$  algebra representations. This setup allows us to assign an arbitrary spin to the emergent low-energy excitations, whose band structures display multiple layered Dirac cones at four isolated points in the first Brillouin zone, termed Dirac points. Such band structure gives rise to exotic properties, e.g., a rich anomalous quantum Hall effect and Klein multi-refractive tunnelling. The shape of the cones, i.e., the different Fermi velocities of quasi-particles are completely fixed by the  $\mathfrak{su}(2)$  representation. In this work, we show how to relax the above constraint, providing a playground for simulations of high energy phenomena such as neutrino oscillations [7] in Lorentz and CPT breaking/no breaking scenarios [8–10]. A related proposal of a similar mechanism in  $^3\text{He}$  appeared in [11].

**The model.** For an optical square superlattice filled with multi-component alkali fermions, the Hamiltonian is [12]

$$H = H_t + H_o = - \sum_{\mathbf{r}, \mathbf{v}} \sum_{\tau, \tau'} t_{\mathbf{v}} [\mathbb{T}_{\mathbf{v}}]_{\tau' \tau} c_{\mathbf{r}+\mathbf{v}, \tau'}^\dagger c_{\mathbf{r}, \tau} + \text{H.c.} + \sum_{\mathbf{r}} \sum_{\tau, \tau'} [\mathbb{O}]_{\tau' \tau} c_{\mathbf{r}, \tau'}^\dagger c_{\mathbf{r}, \tau}, \quad (1)$$

where  $H_t$  describes the nearest-neighbor hopping dynamics,  $H_o$  the on-site dynamics, and  $c_{\mathbf{r}\tau}^\dagger (c_{\mathbf{r}\tau})$  are fermionic creation (annihilation) operators with an internal index  $\tau$ . The optical potential is assumed to be deep enough so that free hopping due to kinetic energy is suppressed. The tunneling is laser-assisted by Raman transitions where its amplitude along the  $\mathbf{v} = x, y$  direction is described by a spin-dependent operator  $\mathbb{T}_{\mathbf{v}}$ . For a detailed discussion of experimental realizations we refer the reader to Refs. [6, 12]. In such laser-assisted hopping schemes, each of the matrix elements of the hopping operators is realized via an effective four-photon process, where the spin of the atom can be flipped with at most  $|\Delta m_F| = 4$  [12]. As explained below, we demand non-zero elements of the hopping matrices only around the diagonal, i.e., with a superdiagonal and a subdiagonal which involve only  $|\Delta m_F| = 1$ .

We first consider the tunneling dynamics with  $H_t$ . In momentum space  $H_t$  reduces to  $H = \sum_{\mathbf{k}} \Psi^\dagger(\mathbf{k}) H(\mathbf{k}) \Psi(\mathbf{k})$  where  $H(\mathbf{k}) = -\sum_{\mathbf{v}} 2t_{\mathbf{v}} \mathbb{T}_{\mathbf{v}} \cos(k_{\mathbf{v}})$ , the spinor  $\Psi(\mathbf{k}) = (c_{\mathbf{k}1}, \dots, c_{\mathbf{k}N})^t$  contains the fermionic operators, and  $k_{\mathbf{v}}$  is in units of the lattice spacing. When the hopping operators  $\mathbb{T}_{\mathbf{v}}$  are tuned according to the  $n$ -dimensional representation of the  $\mathfrak{su}(2)$  Lie algebra, namely,  $\mathbb{T}_x = \Sigma_x$  and  $\mathbb{T}_y = \Sigma_y$  which fulfill the corresponding algebra  $[\Sigma_z, \Sigma_{\pm}] = \pm 2i\Sigma_{\pm}$  and  $[\Sigma_x, \Sigma_y] = 2i\Sigma_z$  where  $\Sigma_{\pm} = \Sigma_x \pm i\Sigma_y$ , then the low energy excitations of the system are Dirac-Weyl fermions with integer or half-integer spin depending on whether  $n$  is odd or even. A simple representation of  $\Sigma_x$  and  $\Sigma_y$  for spin  $s$  with  $n = 2s + 1$  which generalizes the Pauli representation for spin 1/2, can be expressed in terms of a  $(n-1)$ -vector  $\boldsymbol{\rho}_n \equiv (\rho_1, \rho_2, \dots, \rho_{n-1})$  where  $\rho_j = \sqrt{j(n-j)}$  such that  $\Sigma_x = \{\text{Superdiag}\{\rho_j\}, \text{Subdiag}\{\rho_j\}\}$  and  $\Sigma_y = \{\text{Superdiag}\{-i\rho_j\}, \text{Subdiag}\{i\rho_j\}\}$ ,  $j = 1, \dots, n-1$ .

However, it is worth noticing that for any real vector  $\boldsymbol{\rho}$ ,  $\mathbb{T}_x = \{\text{Superdiag}\{\rho_j\}, \text{Subdiag}\{\rho_j\}\}$  and  $\mathbb{T}_y = \{\text{Superdiag}\{-i\rho_j\}, \text{Subdiag}\{i\rho_j\}\}$ , the location of the Dirac points of  $H(\mathbf{k})$  does not change because the spectrum is  $E(\mathbf{k}) = \epsilon_{\boldsymbol{\rho}} |\mathbf{g}_{\mathbf{k}}|$  where  $\epsilon_{\boldsymbol{\rho}}$  are the eigenvalues of the  $\mathbb{T}_{\mathbf{v}}$  matrix with  $\mathbf{v} = x, y$  and  $\mathbf{g}_{\mathbf{k}} = (2t_x \cos k_x, 2t_y \cos k_y, 0)$ . This observation is crucial as the *leitmotif* of the paper is to preserve the stability of the Dirac points while relaxing the integer or half-integer spin structure such that we can construct arbitrary

effective speeds of light in the emergent quasi-relativistic scenario. To this aim it is essential to keep the off-diagonal shape of the hopping matrices while allowing  $\rho_j$  to be any real value [13]. Properties that depend on the topological aspects of the system such as the topologically invariant Berry phase, the topological charge and the Hall plateaus will consequently not change, while properties depending on local aspects of the system such as the butterfly nature of the spectrum and the Klein multirefringent tunnelling will change [6]. The resulting spectrum at each Dirac point will be a collection of Dirac fermions with tunable effective speeds of light and a topological charge  $N$  equal to the number of the layers.

As an example, we consider a double layered Dirac cone structure with tunable Fermi velocity for each component. We parametrize  $\mathbf{p}_4$  as  $\rho(\sin\theta\cos\phi, \sin\theta\sin\phi, \cos\theta)$ . The corresponding spectrum is of the form  $\varepsilon = \rho\sqrt{1 \pm \chi/2}/\sqrt{2}$ , where  $\chi = \sqrt{3 + \cos 2\phi + \cos 4\theta - \cos 2\phi \cos 4\theta}$ . Interestingly, a birefringent breakup of the doubly degenerate Dirac cones into cones with different speeds of light have also been discussed in quite a different setup with cold atoms [14]. It is worth stressing that our setup allows a breakup, or indeed a coalition, of *any* number of Dirac fermions and can lead to super-Dirac fermions which consist of multiple degenerate cones with any integer number of topological charges. For example, when  $\chi = 0$  the two layered cones collapse into a single degenerate one with topological charge  $N = 2$ . This is also the mechanism for mixing the different Dirac species when on-site dynamics is introduced. The  $N = 3$  situation, on the other hand, can be used to mimic the three families of fermions in particle physics. These hopping matrices considered above can also be seen as generalized spin-orbit coupled systems (see [15] for a recent realization in a Bose-Einstein condensate).

#### Mixing of Dirac species and Topological Phase Transitions.

While the hopping Hamiltonian  $H_t$  in Eq. (1) allows us to create a collection of Dirac fermions at the *same* location in momentum space with tunable Fermi velocities, a constant on-site term  $H_o$  gives an effective mixing of the different Dirac species. This mixing mechanism is fundamentally different compared to the mixing mechanism in graphene. In graphene the Dirac fermions are located at *different* sites  $K_{\pm}$  in the momentum space. A commensurate perturbation  $G = K_+ - K_-$  introduced by lattice distortions is needed to mix the Dirac fermions (see [16, 17] for a discussion of the chiral mixing in graphene by Kekule texture when constructing the chiral gauge theory of graphene). Furthermore, opening a gap in monolayer graphene is difficult, too. Our setup allows mixing of any number of Dirac fermions of the same chirality, and to open up gaps by the on-site microwave Raman transitions.

We now consider the mixing of triple degenerate Dirac cones with a topological charge of  $N = 3$  at a single Dirac point  $\mathbf{K}_W = \frac{\pi}{2}(1, 1)$ , i.e., at the same location in momentum space. We write the constant mixing term - a special case of the  $\odot$  of Eq. (1) - in the form of  $\mathbf{h} \cdot \boldsymbol{\sigma}$  where  $\mathbf{h} = (h_1, h_2, h_3)$ , and  $\boldsymbol{\sigma} = (\sigma_x, \sigma_y, \sigma_z)$  is a vector of Pauli matrices. The unperturbed case  $\mathbf{h} = 0$  corresponds to  $\mathbf{p}_6 = (1, 0, 1, 0, 1)$ . The result is a combination of mixing and splitting of the Dirac points,

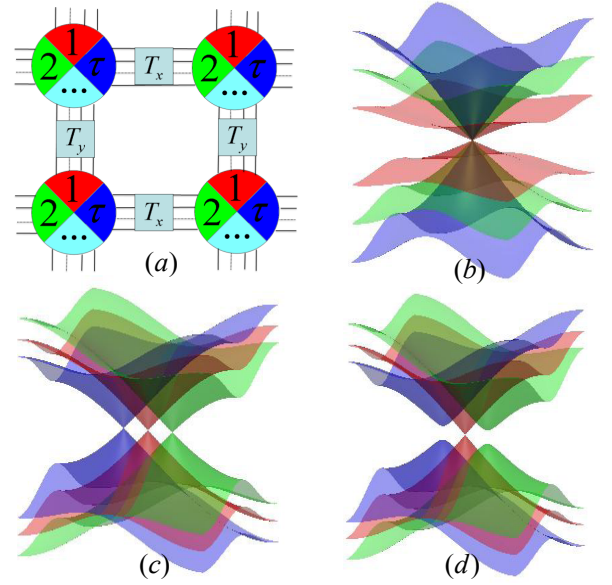


Figure 1. Setup and typical band structures considered in the text. (a) Schematic illustration of the optical lattice and its tunneling mechanism. (b) The triple layered Dirac cone with three different effective speeds of light. (c) The splitting of triple degenerate Dirac cones. (d) Gap opening of the cones as in (c). The band structure in (c) is used to simulate neutrino oscillations as discussed in the text.

which are the paradigm of topological quantum phase transitions (TPT). The corresponding Hamiltonian near the Dirac point is

$$H_m(\mathbf{k}) = \begin{bmatrix} \mathbf{g}_k \cdot \boldsymbol{\sigma} & 0 & 0 \\ 0 & (\mathbf{g}_k - \mathbf{h}) \cdot \boldsymbol{\sigma} & 0 \\ 0 & 0 & (\mathbf{g}_k - \mathbf{h}') \cdot \boldsymbol{\sigma} \end{bmatrix}. \quad (2)$$

The spectrum is given by  $E_1 = \pm|\mathbf{g}_k|$ ,  $E_{2(3)} = \pm|\mathbf{g}_k - \mathbf{h}^{(i)}|$ . This concise expression provides a convenient way to control the position of the split Dirac points in the Brillouin zone. While  $h_1^{(i)}$  and  $h_2^{(i)}$  control the positions of the split Dirac points,  $h_3^{(i)}$  controls the gap of the energy spectrum (see Fig. 1). By requiring  $E = 0$  and setting  $h_3 = 0$  for the time being, the split Dirac points are determined by the conditions  $2t_x \cos k_x - h_1^{(i)} = 0$  and  $2t_y \cos k_y - h_2^{(i)} = 0$ . In principle,  $\mathbf{h}^{(i)}$  may be tuned to appropriately large values to create marginal Dirac points with topological charge  $N = 0$  by considering the Dirac points of opposite chirality. The applications of such a scenario go beyond the realm of condensed matter [11]. However, in what follows we will focus on perturbative splitting.

*Neutrino oscillation.* Neutrino oscillations (NO) are considered by many as a possible window for physics beyond the Standard Model. The most accepted mechanism to explain such oscillations is in terms of the nontrivial mass term matrix. The Lagrangian density describing the flavour states  $\mathbf{v}_f^T = (v_e, v_\mu, v_\tau)$  with a mixed mass term  $M$  is  $\mathcal{L} = \bar{\mathbf{v}}_f(x)(i\gamma^\mu \partial_\mu - M)\mathbf{v}_f(x)$ . The flavour of the neutrino oscillates as it propagates since the flavour eigenstates, which are the eigenstates of the weak interactions in conjunction

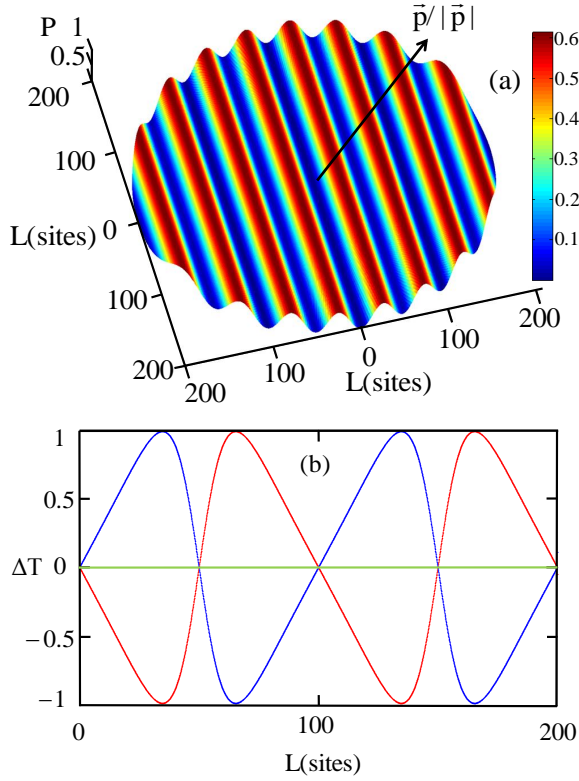


Figure 2. Anisotropic quasi-neutrino oscillations and T-violations in optical lattice with mixing angles  $(\theta_{12}, \theta_{13}, \theta_{23}) = (1/4, 1/4, 1/4)\pi$  and splitting  $\mathbf{h} = \pm 0.01(2\pi)(1, 0)$ . (a) The oscillations of the probability  $P(\nu_e \rightarrow \nu_\mu)$  with the directional vector  $\hat{p}$  of the momentum where the CP-violation phase is  $\delta = 0$ . (b) The T-violation behaviour with  $\delta = \pi/2$  (red),  $3\pi/2$  (blue),  $0, \pi$  (green), where  $\Delta T = (P(\nu_e \rightarrow \nu_\mu) - P(\nu_\mu \rightarrow \nu_e)) / (P(\nu_e \rightarrow \nu_\mu) + P(\nu_\mu \rightarrow \nu_e))$ .

with a particular flavour of a charged lepton, do not coincide with their mass eigenstates with a definite mass and energy. In general, the weak interaction flavour eigenstates can be represented as a coherent linear superposition of the mass eigenstates,  $\mathbf{v}_f = U\mathbf{v}_m$  where  $\mathbf{v}_m^T = (v_1, v_2, v_3)$  describes the state with definite masses and  $U$  is the unitary transform matrix that diagonalizes the mixing mass matrix  $M$ , known as the Pontecorvo-Maki-Nakagawa-Sakata (PMNS) lepton mixing matrix - the counterpart of the Cabibbo-Kobayashi-Maskawa mixing matrix in the quark sector. For all currently observed NO, the corresponding masses are less than 1eV and the energies are at least  $E \gtrsim 1\text{MeV}$ , with a Lorentz factor greater than  $10^6$  in all cases. In this ultrarelativistic limit the energy is given by  $E_i = (p^2 c^2 + m_i^2 c^4)^{1/2} \simeq E + m_i^2 c^4 / 2E$ . The time-dependent mass states are  $|\nu_i(t)\rangle = \exp[-iE_i t / \hbar] |\nu_i\rangle$ , thus  $\mathbf{v}_f(t) = UTU^\dagger \mathbf{v}_f(0)$  where  $T = \text{diag}\{\exp[-iE_1 t / \hbar], \exp[-iE_2 t / \hbar], \exp[-iE_3 t / \hbar]\}$  is the time evolution matrix, i.e.,  $P(\nu_\alpha \rightarrow \nu_\beta) = |\sum_j U_{\alpha j} U_{\beta j}^* \exp[-i \frac{m_j^2 c^4}{2E} t]|^2$ , which shows that the neutrino flavour changes with time. The NO are attributed to the mass difference between the mass states [7]. The mechanism to generate such mass - or any other mixing term - implies

an extension of the Standard Model. The question of which mechanism is the best is still not completely settled.

*NO as TPT in optical lattices.* An analogue of NO can be engineered in optical lattices. The simple model of Eq. 2 is the starting point to capture the essence of 3 species' mixing [18]. For sake of simplicity, we consider  $\mathbf{h} = -\mathbf{h}'$ , and isotropic Fermi velocity, i.e., the effective speed of light  $c_l = t_x = t_y$ . Indeed, an ultra-relativistic limit for coupled pseudo-particles with a *direction dependent mass* can be achieved in the limit of small  $\mathbf{h} = (h_1, h_2, 0)$ . For  $|\mathbf{h}| \ll |\mathbf{g}_\mathbf{k}| \simeq c_l |\mathbf{p}|$ , where  $\mathbf{p} \equiv (\mathbf{K}_W - \mathbf{k})$ , the dispersion relations for the 3 species become:  $E_1 = c_l |\mathbf{p}|$ ,  $E_2 = c_l (|\mathbf{p}| - \hat{p} \cdot \mathbf{h}) = E_1 - \Delta(\hat{p})$  and  $E_3 = c_l (|\mathbf{p}| + \hat{p} \cdot \mathbf{h}) = E_1 + \Delta(\hat{p})$ , where  $\hat{p} \equiv \mathbf{p} / (c_l |\mathbf{p}|)$ . Hence,  $H_m(\mathbf{k})$  of Eq. 2 plays the role of the block diagonal Hamiltonian in the *mass* basis. In fact, to observe NO in the lab we have to implement the Hamiltonian  $H_f(\mathbf{k})$  governing the *flavour* pseudo-particles. In terms of the PMNS mixing matrix  $U$ ,  $H_f(\mathbf{k}) = (U^\dagger \otimes I_2) H_m(\mathbf{k}) (U \otimes I_2) = I_3 \otimes \mathbf{g}_\mathbf{k} \cdot \boldsymbol{\sigma} + M \otimes \mathbf{h} \cdot \boldsymbol{\sigma}$ , where  $I_n$  is the  $n \times n$ -identity matrix, and  $M \equiv U^\dagger \text{diag}\{0, -1, 1\} U$ , i.e.,  $M_{ij} = U_{3j} U_{3i}^* - U_{2j} U_{2i}^*$ . In Lagrangian terms, our 2+1 model is  $\mathcal{L} = \bar{\Psi}_f(x) (i\gamma^\mu \partial_\mu - M\gamma^\mu h_\mu) \Psi_f(x)$  near the Dirac point. Thus the flavour Hamiltonian fits in the family of Eq. 1,  $H_f(\mathbf{k}) = H_t(\mathbf{k}) + H_o(\mathbf{h})$ , with  $H_t(\mathbf{k}) = I_3 \otimes \mathbf{g}_\mathbf{k} \cdot \boldsymbol{\sigma}$  and  $H_o(\mathbf{h}) = M \otimes \mathbf{h} \cdot \boldsymbol{\sigma}$ . Remarkably, while  $H_t(\mathbf{k})$  can be implemented by the triple-layered degenerate Dirac cones as discussed above, the PMNS mixing matrix is completely encoded by the on-site Hamiltonian  $H_o(\mathbf{h})$ , which allows us in principle to simulate any mixing angles and CP-violating phase - the standard parametrization of the PMNS can be found for instance in [7] - by the on-site microwave Raman transitions [12]. As an explicit example, we discuss the simplified case when all the mixing angles are equal to  $\pi/4$  with

$$H_f^{\text{ex}} = \begin{bmatrix} (\mathbf{g}_\mathbf{k} - \cos \frac{\delta}{\sqrt{2}} \mathbf{h}) \cdot \boldsymbol{\sigma} & -i \sin \frac{\delta}{\sqrt{2}} \mathbf{h} \cdot \boldsymbol{\sigma} & \frac{1}{2} \mathbf{h} \cdot \boldsymbol{\sigma} \\ i \sin \frac{\delta}{\sqrt{2}} \mathbf{h} \cdot \boldsymbol{\sigma} & (\mathbf{g}_\mathbf{k} + \cos \frac{\delta}{\sqrt{2}} \mathbf{h}) \cdot \boldsymbol{\sigma} & -\frac{1}{2} \mathbf{h} \cdot \boldsymbol{\sigma} \\ \frac{1}{2} \mathbf{h} \cdot \boldsymbol{\sigma} & -\frac{1}{2} \mathbf{h} \cdot \boldsymbol{\sigma} & \mathbf{g}_\mathbf{k} \cdot \boldsymbol{\sigma} \end{bmatrix}, \quad (3)$$

and  $\delta$  is the CP-violating phase. The quasi-neutrino oscillations are shown in figure 2. In figure 2 (a), the oscillation probabilities for  $\delta = 0$  are plotted against  $\hat{p}$ , showing anisotropic and energy-independent behaviors. The Hamiltonian of Eq. 3 is real, hence invariant under time-reverse symmetry  $T$ . Since the oscillation period is inversely proportional to the splitting, one obtains for a small splitting parameter  $|\mathbf{h}| \sim 0.01(2\pi/a)$ , a period which is of the size of typical lattices. In high energy physics, evidence for NO is presented over a distance  $L \geq 100\text{km}$  and no evidence for oscillations for  $L \leq 1\text{km}$  [7]. In figure 2 (b), the effect of  $\delta \neq 0$  is considered. The Hamiltonian becomes complex and  $T$  is violated. Due to CPT invariance, T-violation is equivalent to CP-violation. The Time-violation behaviour of the transition probability  $P(\Psi_\alpha \rightarrow \Psi_\beta) \neq P(\Psi_\beta \rightarrow \Psi_\alpha)$  is shown for  $\delta = \{0, 1/2, 1, 3/2\}\pi$ . The signature of CP-violation is rather spectacular. In the optical lattice experiment, direct evidences of the above phenomena can be obtained by measuring the different populations in different points of the lat-



tice by the colour resolution or individual atom detection techniques[19, 20].

Our model is Lorentz and CPT conserving if  $\mathbf{h}$  is a Lorentz covariant vector. Indeed, the role of symmetries in the analogue simulation is subtle as they are *artificial*. The Hamiltonian engineered in the lattice is specific for a certain reference frame (or gauge). To consider transformed Hamiltonians in other frames implies physical modifications of the experimental apparatus - for similar discussions of gauge symmetries see [21]. In practise, we can choose how  $\mathbf{h}$  transforms. For instance, we can treat it as a constant vector and reproduce one of the Lorentz and CPT violating NO terms, as discussed in extensions of the Standard Model [8]. The simulation of NO in optical lattices is not only a relevant exercise in order to show the vast possibilities of ultracold atom technology, but it also opens the way to study the effect of novel physics. In particular, optical lattices can be ideal for simulating new flavour couplings originated by strong coupling in a controllable way.

*Engineering exotic particle dispersions.* Modifications of the particle dispersion relations have attracted great interests in both condensed matter and high energy physics. The Dirac fermion seen in graphene and multicomponent atoms in optical lattices for instance, are examples of engineered dispersion relations in a condensed matter setting. It has also been shown that the so called semi-Dirac fermions with linear dispersion in one direction and quadratic dispersion in the other can be made [22]. On the other hand, in high energy physics, modifications of the energy momentum dispersion relations at the Planck scale is a common approach to reconcile the paradox between Lorentz symmetry and finite resolution of the spacetime points in quantum gravity models [23]. Since the spectrum of the low energy excitations in the vicinity of the multiple degenerate Dirac point depends on symmetry, one may obtain several Dirac fermions if there is a particle-hole symmetry, or exotic fermion dispersions at low energy when there is mixing between the different Dirac species [24]. The multi-layered Dirac cones scenario provides a convenient way to engineer the particle dispersion to have any power of the momentum when introducing proper mixing among the different Dirac species. As discussed in [24], the Hamiltonian to achieve this is  $\mathcal{H}(\mathbf{p}) = \{\text{superdiag}\{g\sigma^+\}, \text{diag}\{\mathbf{p} \cdot \boldsymbol{\sigma}\}, \text{subdiag}\{g\sigma^-\}\}$  which will mix the  $N$  Dirac species and give the spectrum  $E \sim p^N$ . The optical lattice with multicomponent atoms provides a feasible realization of such exotic kinds of particle dispersion by using the  $\text{diag}\{\mathbf{p} \cdot \boldsymbol{\sigma}\}$  term from the hopping dynamics and  $\text{superdiag}\{g\sigma^+\}$  and  $\text{subdiag}\{g\sigma^-\}$  terms from the on-site dynamics.

*Conclusions.* We have shown how multiple-layered Dirac cones can be used to simulate various phenomena from the realm of particle physics. The advances in manipulation of cold atoms in optical lattices can provide us with a fascinating possibility to test these ideas. We believe the interplay between condensed matter, particle physics and quantum simulations could lead us to new paradigms, much in the spirit of fundamental theories as emerging phenomena [25].

*Note added.* Once this work was completed, [26] appeared

proposing an ion trap simulator of NO in 1+1 dimensions.

Z.L. acknowledges the support from SUPA. A.C. and M.L. acknowledge funding from the Spanish MEC projects TO-QATA (FIS2008-00784), QOIT (Consolider Ingenio 2010), ERC Advanced Grant QUAGATUA, EU STREP NAME-QUAM. M.L. acknowledges the financial support of Alexander von Humboldt Foundation. P.Ö acknowledges support from the Carnegie Trust for the Universities of Scotland.

- 
- [1] R.P. Feynman, Int. J. Theor. Phys. **21**, 467 (1982).
  - [2] I. Bloch *et al*, Rev. Mod. Phys. **80**, 885 (2008).
  - [3] I. Buluta and F. Nori, Science **326**, 108 (2009).
  - [4] A. H. Castro Neto *et al*, Rev. Mod. Phys. **81**, 109 (2009).
  - [5] M. Z. Hasan and C. L. Kane, Rev. Mod. Phys. **82** 3045 (2010); X.-L. Qi and S.-C. Zhang, arXiv:1008.2026 (2010).
  - [6] Z. Lan *et al*, arXiv:1102.5283 (2011).
  - [7] H. Nunokawa *et al*, Prog. Part. Nucl. Phys. **60**, 338 (2008).
  - [8] V. A. Kosteletsky and M. Mewes, Phys. Rev. D **69**, 016005 (2004).
  - [9] F. R. Klinkhamer, JEPT letters, **79**, 451 (2004).
  - [10] F. R. Klinkhamer and G. E. Volovik, Int. J. Mod. Phys. A, **20**, 2795 (2005).
  - [11] G. E. Volovik, *The Universe in a helium droplet* (Oxford, UK: Oxford University Press, 2003).
  - [12] L. Mazza *et al*, arXiv:1105.0932 (2011).
  - [13] For  $\mathbb{T}_x = \{\text{Superdiag}\{\rho_j\}, \text{Subdiag}\{\rho_j\}\}$ , the spectrum is determined by the zeros of  $\det(\mathbb{T}_x - \epsilon \mathbb{I}^{(n)}) = P_n(\epsilon)$  where  $\epsilon$  is the eigenvalue. Consequently we get the recurrence relation  $P_{n+1}(\epsilon) = -\epsilon P_n(\epsilon) - \rho_n^2 P_{n-1}(\epsilon)$ , with the initial conditions  $P_0 = 1$  and  $P_1 = -\epsilon$ . By induction we get  $P_n(\epsilon) = f_n(\epsilon^2)$ ,  $n \in \{2k, \forall k \in \mathbb{Z}_+\}$  and  $P_n(\epsilon) = \epsilon g_n(\epsilon^2)$ ,  $n \in \{2k+1, \forall k \in \mathbb{Z}_+\}$ , which demonstrates the particle-hole symmetry of  $\mathbb{T}_x$ , and the zero energy flat band for odd dimensional representations. It is straightforward to show that  $\mathbb{T}_y$  has the same eigenvalues as  $\mathbb{T}_x$  as they share the same characteristic polynomial.
  - [14] M. P. Kennett *et al*, arXiv:1011.1502 (2010).
  - [15] Y.-J. Lin *et al*, Nature, **471**, 83 (2011).
  - [16] C. Hou *et al*, Phys. Rev. Lett. **98**, 186809 (2007).
  - [17] R. Jackiw and S.-Y. Pi, Phys. Rev. Lett. **98**, 266402 (2007).
  - [18] The mechanism of NO cannot be achieved by introducing directly mass terms in the 2+1 Dirac Hamiltonian because in the optical lattice the relativistic Dirac physics emerges only in the neighborhood of the Dirac points, and they are destroyed by the mass term. In other words, the massive Dirac equation is a good description of the quasi-particle dynamics only in the non-relativistic limit, i.e. when Dirac Hamiltonian reduces to the Schrödinger one. An alternative, as shown in the main text, is to trade off Dirac points' splitting for mass splitting.
  - [19] W. S. Bakr *et al*, Nature **462**, 74 (2009).
  - [20] J. F. Sherson *et al*, Nature **467**, 68 (2010).
  - [21] O. Boada *et al*, New J. Phys. **12**, 113055 (2010).
  - [22] P. Delplace and G. Montambaux, Phys. Rev. Lett. **82**, 035438 (2010).
  - [23] A. S. Sefiedgar *et al*, Phys. Lett. B **696**, 119 (2011).
  - [24] T. T. Heikkilä and G. E. Volovik, JEPT letters, **92**, 681 (2010).
  - [25] M. Levin and X. -G. Wen, Rev. Mod. Phys. **77**, 871 (2005).
  - [26] C. Noh *et al*, arXiv:1108.0182 (2011).